Structure and phase transitions of single-wall carbon nanotube bundles under hydrostatic pressure

X. H. Zhang,[1] D. Y. Sun,[2] Z. F. Liu,[3] and X. G. Gong[1,2]
[1]*Surface Physics Laboratory (National Key Laboratory), Fudan University, Shanghai 200433, People's Republic of China*
[2]*Institute of Solid State Physics, Chinese Academy of Sciences, Hefei 230031, People's Republic of China*
[3]*Department of Chemistry, The Chinese University of Hong Kong, Shatin, Hong Kong, People's Republic of China*
(Received 6 June 2003; revised manuscript received 10 March 2004; published 30 July 2004)

We have studied the structures of single-wall carbon nanotube bundles with and without hydrostatic pressure by using constant pressure molecular dynamics methods. The structure is found to be strongly dependent on the symmetry of the tubes, and only $(6n, 6n)$ tubes could be assembled into an ideal hexagonal lattice. With increasing pressure, all tube lattices undergo a structure transition, while the transition pressure varies with the symmetry and radius of the tube.

DOI: 10.1103/PhysRevB.70.035422 PACS number(s): 61.48.+c, 61.50.Ks, 71.15.Pd, 73.63.Fg

I. INTRODUCTION

Carbon nanotubes have been studied extensively in the last decade and have been found to have extraordinary properties.[1] Of great interest is the mechanical properties of single-wall carbon nanotube bundles (SWCNTB's) under pressure.[2–17] Experimental studies on SWCNTB's have shown evidence of pressure-induced phase transition.[4–9] Several high-pressure Raman investigations on SWCNTB's were carried out recently.[4,5] All of them showed that the vibrational frequency of the radial modes shifts up and the Raman intensity reduces dramatically beyond a few GPa. The changes are reversible upon unloading the pressure. These results strongly indicate a structural transition. However, the transition pressure varies in a rather large range from 1.7 GPa to 10 GPa. A recent x-ray diffraction study on SWCNTB's under pressure[7] found a reversible disappearance of the triangular lattice at ~1.5 GPa, if the pressure was unloaded from less than 4 GPa. Accompanying polygonization of SWCNTB's, a discontinuous change in electrical resistivity was observed at 1.5 GPa.[8] Beyond 5 GPa the x-ray results showed an irreversible change. The optical absorption spectra[9] also showed reversibility up to 4.1 GPa. However, an *in situ* x-ray diffraction investigation on SWCNTB's under quasihydrostatic pressure found that the lattice of the SWCNTB's continues to exit up to ~10 GPa.[11]

Structural transition of (10,10) SWCNTB's from hexagonal to monoclinic phase was observed in molecular dynamics simulation with the force field.[7] Very recently, *ab initio* calculations[17] showed that (10,10) SWCNTB's undergo a phase transition above 1 GPa, while in contrast (12,12) SWCNTB's gradually polygonize with increasing pressure up to 6 GPa without any phase transition. These theoretical studies provided important information to understand the behavior of nanotube bundles under external pressure, although many problems are still open and worthy of further investigation. For instance, the physical properties of tubes, such as the transition pressure, are closely related to the tube radius and lattice symmetry. However, the dependence of the transition pressure on the structure of the lattice is not clear, and the tube-tube interactions in the lattice have still not been revealed. Although the pressure-induced phase transition has been confirmed by experiments and recent theoretical simulation, the changes in structure and mechanical properties due to the phase transition has not been well studied yet. Very recently, pressure-induced circular-elliptical shape transition of an isolated single-wall carbon nanotube has been predicted theoretically by Sun *et al.*[18] with a constant-pressure molecular dynamics method developed for finite systems.[19] It is interesting to compare the different behaviors between an isolated single-wall carbon nanotube and single-wall carbon nanotube bundles, which could be helpful in understanding the role of the tube-tube interaction.

In this paper, (6,6), (8,8), (10,10), (12,12), (15,15), (24,0), and (30,0) SWCNTB's under hydrostatic pressure are studied by using Parrinello-Rahman constant-pressure molecular dynamics simulations.[20] The results show a transition for each SWCNTB, and the transition pressure and the structural changes depend on the symmetry of tubes and the their radius as well.

II. CALCULATION DETAILS

The present simulation is set for the lattice of SWCNTB's, with all the tubes assembled in hexagonal symmetry. We use periodic boundary conditions in all three dimensions for infinitely long tubes without any caps. There are 20 layers of atoms in the axial direction (Z), while a 4×4 supercell, consisting of 16 carbon nanotubes, is arranged in the X-Y plane. For each type of SWCNTB, the lattice constant is optimized, together with the relative orientation of adjacent tubes and interatomic distances, by minimizing the total energy of the simulation cell. In order to simulate the structural changes under pressure, we use the Parrinello-Rahman constant-pressure molecular dynamics method[20] and steepest-descent method to obtain the stable structure. The covalent interactions between carbon atoms are simulated by an empirical Tersoff-Brenner many-body potential[21,22] with the parameters given by Brenner,[22] which has been extensively used to model diamond, graphite, carbon nanotubes, and many hydrocarbon complexes.[23–28] The intertube and intratube van der Waals interactions are modeled in the usual

TABLE I. Lattice parameters without external pressure, critical transition pressures (P_t), and bulk moduli (B) of SWCNTB's. a and b are the lattice constants of SWCNTB's, and α is the angle between the two lattice vectors. t is the shortest intertube distance. The ratio $\eta = R_s/R_0$ is defined as the deformation of a tube, where R_s is the shortest radial dimension and R_0 is the radius of an isolated tube.

SWCNTB	R_0 (Å)	t (Å)	a (Å)	b (Å)	α (°)	η	Cross section of shape before transition	P_t (GPa)	B (GPa)
(6,6)	4.07	3.23	11.44	11.44	120.0	0.992	Hexagonal	5.70	68
(8,8)	5.42	3.04	13.88	13.81	120.1	0.993	Oval	1.60	36
(10,10)	6.78	3.07	16.10	16.48	117.8	0.961	Oval	0.70	24
(12,12)	8.14	3.07	19.06	19.06	120.0	0.982	Hexagonal	0.80	25
(24,0)	9.40	3.16	19.41	21.67	111.2	0.864	Oval	0.25	11
(15,15)	10.18	3.13	22.84	22.85	120.0	0.968	Nearly hexagonal	0.80	20
(30,0)	11.75	3.23	23.55	25.86	111.3	0.865	Oval	0.15	9

way by the 6–12 Lennard-Jones potential[29,30] with a cutoff distance of 15 Å. The intratube van der Waals interaction is included when the tube is compressed to an oval shape.

III. RESULTS AND DISCUSSIONS

Seven different lattices assembled by (6,6), (8,8), (10,10), (12,12), (15,15), (24,0), and (30,0) SWCNTB's, respectively, with the radius ranging from ~4 to 12Å, are studied in the present simulation.

In order to obtain the lattice constant at zero pressure, the total energy of the tubes in the simulation cell is minimized by relaxing all the atomic positions and the shape of the cell. The lattice constants and structural data obtained are listed in Table I.

The intertube van der Waals interaction drives the shape of the cross section of tubes in the lattice changing from circular to hexagonal or oval, even without any external pressure. Among these tube bundles, we find two different shapes for the cross section, hexagonal/nearly hexagonal shape only for (6,6), (12,12), and (15,15) SWCNTB's, and oval shape for (8,8), (10,10), (24,0), and (30,0) SWCNTB's. For the (6,6) and (12,12) SWCNTB lattices, the lattice constants a and b are equal, and the angle between two lattice vectors is 120°, showing an ideal hexagonal lattice symmetry. Similarly, for the (15,15) SWCNTB lattice, the cross section is very close to the hexagonal shape, and the difference between two lattice constants is very small.

However, for tubes with an oval shape, a significant distortion from the hexagonal lattice (see Table I) exists. The lattice constants a and b are obviously different, corresponding to a monoclinic structure. The difference between a and b increases with increasing tube radius. For the (10,10) SWCNTB's, the lattice constants a and b are 16.48 Å and 16.10 Å, respectively, the ratio of the long and short radius is close to 1.02, and the angle between two lattice vectors becomes 116.8°. These agree well with the experimental observation[7,8] and *ab initio* results.[17] The obtained intertube distance is about 3.1 Å, which is also in agreement with available data.[7,17] For larger tubes, such as (24,0) and (30,0) SWCNTB's, a larger distortion has been observed. The ratio of the long to short radius is found to be 1.08, and the angle between two lattice vectors is also larger than that in (10,10) SWCNTB's. A parameter $\eta = R_s/R_0$ is defined to describe the tube deformation induced by the intertube interaction, where R_s and R_0 are the shortest axis of the cross section and the radius of the tube, respectively. From Table I, it can be seen that such deformation also increases with tube radius.

The shape of the tube cross section is determined by the symmetry of the tube. According to Damnjanović *et al.*,[31] the symmetry group of individual single-wall carbon nanotubes (n,n) and $(n,0)$ is $T_2^1 D_{nh}$. Present simulations show that under pressure the symmetries of T_2^1 and σ_h are retained. However, the symmetry of the cross section is reduced from D_n to C_6 for (6,6) and (12,12) SWCNTB's, to C_3 for (15,15) SWCNTB, and to C_2 for (8,8), (10,10), (24,0), and (30,0) SWCNTB's. A necessary condition to form an ideal hexagonal lattice is that the tube itself has a C_6 rotational axis, as required by packing tubes in the hexagonal lattice. This is true for (6,6) and (12,12) SWCNTB lattices, in which an exact hexagonal lattice is formed. For (15,15) SWCNTB which has C_3 symmetry, the equilibrium structure of the tubes shows a distorted hexagon, with two different lengths of the lattice vectors in the unit cell, which leads to slightly different lattice constants a and b, as shown in Table I.

All the zigzag tubes in the lattice show an oval-like shape, independent of their symmetry. To answer why the zigzag tubes cannot get the hexagonal shape while the armchair tubes with C_6 rotational axis can, one needs to explore the atomic structure and the relative orientation between neighboring tubes. In graphite, the adjacent layers are shifted each other to increase the attractive interlayer van der Waals interaction. A similar situation occurs between two adjacent tubes. Carbon tubes in the lattice can rotate in respect to each other to increase the interaction between neighboring tubes. In fact, the circular tubes can deform their shape to increase the interaction between the flattened planes, like two graphite planes. The relative atomic structures between neighboring tubes are schematically shown in Fig. 1. For the armchair (n,n) tubes [Fig. 1(a)], two graphitelike layers on neighboring tubes shift $1/3$ period to reach the maximum interaction position, which can be completed by rotating $2\pi/3n$. All the neighboring tubes are located in an energetically proper position simultaneously. While for the zigzag tubes [Fig. 1(b)], the graphitelike layers can only reach the position with a maximum interaction by shifting $1/2$ period. It is impossible

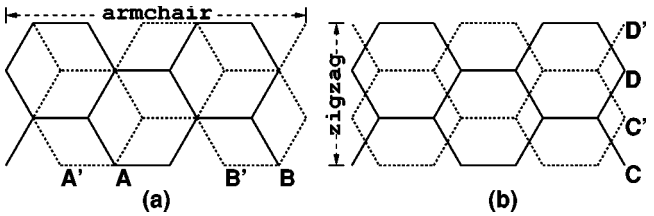

FIG. 1. Schematic illustration of the interface structure of the neighboring tubes in SWCNTB lattices. Solid lines represent one graphitelike plane and the dashed lines another graphitelike plane of the neighboring tube. Along the armchair direction, the lattice slides 1/3 period (AB in one plane and $A'B'$ in another), and along the zigzag direction, the lattice slides 1/2 period along the perpendicular direction (CD in one plane and $C'D'$ in another).

for all the tubes in the lattice to be located at the proper position to maximize the interaction between adjacent tubes. Therefore, the interaction for any tube in the lattice with all six neighbors cannot be hexagonal, making the zigzag tube oval-like.

Present simulation shows that all SWCNTB lattices undergo a pressure-induced structural phase transition, as the cross section of each nanotube changes from circular to elliptic (oval). The obvious discontinuity appears in the dependence of pressure versus the reduced volume, as shown in Fig. 2, which confirms the phase transition. At low pressure, i.e., before the transition, the bulk modulus is of the same order of magnitude as that of Lu[32] and Reich.[16]

The simulation also shows that the transition pressure depends on both the tube radius and the tube symmetry. Figure 3 presents the transition pressure as a function of radius. It can be seen that the transition pressures are strongly dependent on the radius of the tube. Similar to isolated single-wall carbon nanotubes,[18] the transition pressure can be well fitted to $\sim 1/R^3$ for the SWCNTB lattices assembled with oval-like tubes. For comparison, we also show the transition pressure for isolated carbon nanotubes in Fig. 3. One can see that, except for the tubes with a symmetry approximately matched

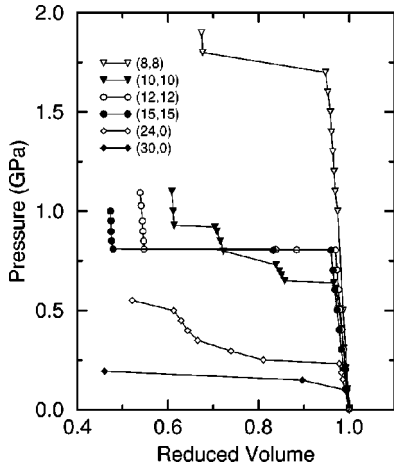

FIG. 2. Pressure vs volume for SWCNTB's. The discontinuity of each curve suggests that a phase transition occurred. Due to its much larger transition pressure, the result of the (6,6) SWCNTB lattice is not shown. Lines are shown to guide the eyes.

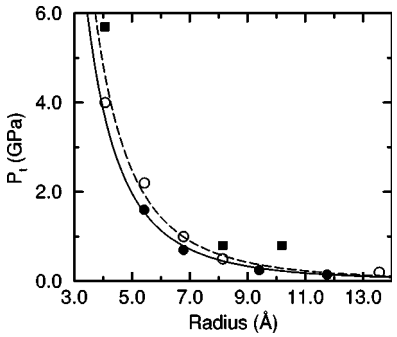

FIG. 3. Transition pressure P_t vs the radius of tube. (6,6), (12,12), and (15,15) SWCNTB lattices (solid squares) have larger transition pressures than those of isolated single-wall carbon nanotubes, while (8,8), (10,10), (24,0), and (30,0) SWCNTB lattices (solid circles) have the lower ones. The blank circles are the transition pressures of (6,6), (8,8), (10,10), (12,12), and (20,20) isolated SWCNTB's (Ref. 18), respectively. The transition pressure can be well fitted to $\sim 1/R^3$ for the solid or blank circles.

to the lattice symmetry, the transition pressure for SWCNTB's is slightly smaller than that of the isolated tubes. This means that the intertube interaction can decrease the phase transition pressure, which is dominated by the properties of individual tubes. However, for the $T_2^1C_{6h}$ and $T_2^1C_{3h}$ SWCNTB lattices, the local structure is well matched between neighboring tubes, and the phase transition pressures of (6,6), (12,12), and (15,15) SWCNTB lattices are higher than the isolated ones, and cannot be fitted to a power dependence.

If the pressure is increased further after the phase transition, the elliptic-like SWCNTB's become more flattened to decrease the volume of the simulation cell in response to the external pressure. It is interesting to note that the volume decreases step by step as can be observed from Fig. 2 for (10,10) and (24,0) SWCNTBs. Figure 4 shows the corresponding structure and shape of SWCNTB lattices under different pressure, where the effect of external pressure on the shape of the tube cross section can be clearly seen. Just after the phase transition, the cross section of the tubes becomes an elongated ellipse. With pressure increasing, it is found that some tubes become more flattened than others, as indicated by A and B, respectively, in Fig. 4(c). Finally all the

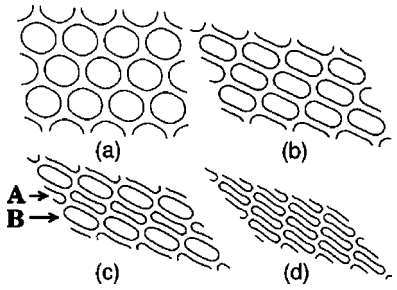

FIG. 4. Snapshots of the cross section of (10,10) SWCNTB's under pressure of (a) 0.6 GPa, (b) 0.7 GPa, (c) 0.85 GPa, and (d) 1.0 GPa. A new metastable state of AB sequence under pressure 0.8–0.93 GPa with A and B representing the dumbbell-like and ellipticlike nanotubes, respectively, is observed.

TABLE II. Energy of A (dumbbell-like nanotubes) and B (ellipticlike nanotubes) in (10,10) SWCNTB's under pressure 0.85 GPa. E, E_1, and E_2 represent energies per atom with both intertube and intratube, with only intratube, and without intertube or intratube van der Waals interactions, respectively. The enthalpies per atom, $H=E+PV$, of A and B are almost the same, which confirms the metastable state of AB sequence under constant pressure.

	Energy/atom (eV)			PV/atom	Enthalpy/atom
	E	E_1	E_2	(eV)	(eV)
A	−7.366	−7.330	−7.318	0.012	−7.354
B	−7.378	−7.342	−7.341	0.021	−7.357
Δ	0.012	0.012	0.023	0.009	0.003

tubes become very flattened, i.e., dumbbell-like, as shown in Fig. 4(d).

The presence of two different structures (A and B) can be qualitatively explained as the following. Since structure A is more compressed and deformed than structure B, the total energy of structure A is higher than that of structure B. However, since the volume of structure A is smaller than structure B, the enthalpies for both structures can be essentially the same. Thus, under the external pressure, both structures can coexist. To confirm this point, we calculate the energies and enthalpies for both structures A and B, which are listed in Table II. As expected, the enthalpies for both structures are nearly the same. We believe that high-resolution experiments on electronic properties can be used to observe such an effect.

IV. SUMMARY

By using Parrinello-Rahman constant-pressure molecular dynamics methods, we have studied the structure of SWCNTB lattices with and without external pressure. We find that, only armchair $(6n,6n)$ tubes can be assembled in exactly hexagonal lattice, while all other tubes with different symmetries can only form a deformed hexagonal lattice. A pressure-induced shape phase transition occurred in SWCNTB's as the shape of the tube cross section changes. The critical transition pressure is strongly dependent on the symmetry and the radius of the nanotubes. For most SWCNTB lattices, the transition pressure is smaller but very close to that of the isolated tubes. For $T_2^1C_{6h}$ and $T_2^1c_{3h}$ SWCNTB lattices, good matching between the local atomic structures of neighboring tubes can enhance the stability of SWCNTB's with respect to the external pressure and can make the transition pressure higher than that of isolated single-wall carbon nanotubes. The present results also show a special metastable state in which the carbon nanotubes have different shapes but similar enthalpy during the transition of SWCNTB lattices.

ACKNOWLEDGMENTS

This work is supported by the National Science Foundation of China, the special funds for major state basic research and CAS projects. Z.F.L. also acknowledges financial support from The Research Grant Council, Hong Kong SAR Government, through Project CUHK 4252/01P.

[1] S. Iijima, Nature (London) **354**, 56 (1991).
[2] J. Tersoff and R. S. Ruoff, Phys. Rev. Lett. **73**, 676 (1994).
[3] S. A. Chesnokov, V. A. Nalimova, A. G. Rinzler, R. E. Smalley, and J. E. Fischer, Phys. Rev. Lett. **82**, 343 (1999).
[4] U. D. Venkateswaran, A. M. Rao, E. Richter, M. Menon, A. Rinzler, R. E. Smalley, and P. C. Eklund, Phys. Rev. B **59**, 10928 (1999).
[5] M. J. Peters, L. E. McNeil, J. P. Lu, and D. Kahn, Phys. Rev. B **61**, 5939 (2000).
[6] R. Gaál, J. P. Salvetat, and L. Forró, Phys. Rev. B **61**, 7320 (2000).
[7] J. Tang, L. C. Qin, T. Sasaki, M. Yudasaka, A. Matsushita, and S. Iijima, Phys. Rev. Lett. **85**, 1887 (2000).
[8] J. Tang, L. C. Qin, T. Sasaki, M. Yudasaki, A. Matsushita, and S. Iijima, J. Phys.: Condens. Matter **14**, 10575 (2002).
[9] S. Kazaoui, N. Minami, H. Yamawaki, K. Aoki, H. Kataura, and Y. Achiba, Phys. Rev. B **62**, 1643 (2000).
[10] C. Q. Ru, Phys. Rev. B **62**, 10405 (2000).
[11] T. Yildirim, O. Gülseren, C. Kilic, and S. Ciraci, Phys. Rev. B **62**, 12648 (2000).
[12] U. D. Venkateswaran, E. A. Brandsen, U. Schlecht, A. M. Rao, E. Richter, I. Loa, K. Syassen, and P. C. Eklund, Phys. Status Solidi B **223**, 225 (2001).
[13] M. J. López, A. Rubio, J. A. Alonso, L. C. Qin, and S. Iijima, Phys. Rev. Lett. **86**, 3056 (2001).
[14] S. M. Sharma, S. Karmakar, S. K. Sikka, P. V. Teredesai, A. K. Sood, A. Govindaraj, and C. N. R. Rao, Phys. Rev. B **63**, 205417 (2001).
[15] S. Rols, I. N. Goncharenko, R. Almairac, J. L. Sauvajol, and I. Mirebeau, Phys. Rev. B **64**, 153401 (2001).
[16] S. Reich, C. Thomsen, and P. Ordejón, Phys. Rev. B **65**, 153407 (2002).
[17] M. H. F. Sluiter, V. Kumar, and Y. Kawazoe, Phys. Rev. B **65**, 161402 (2002).
[18] D. Y. Sun, D. J. Shu, F. Liu, and X. G. Gong (unpublished).
[19] D. Y. Sun and X. G. Gong, J. Phys.: Condens. Matter **14**, L487 (2002).
[20] M. Parrinello and A. Rahman, J. Appl. Phys. **52**, 7182 (1981).
[21] J. Tersoff, Phys. Rev. Lett. **61**, 2879 (1988).
[22] D. W. Brenner, Phys. Rev. B **42**, 9458 (1990).
[23] D. H. Robertson, D. W. Brenner, and J. W. Mintmire, Phys. Rev. B **45**, 12592 (1992).
[24] B. I. Yakobson, C. J. Brabec, and J. Bernholc, Phys. Rev. Lett. **76**, 2511 (1996).
[25] M. B. Nardelli, B. I. Yakobson, and J. Bernholc, Phys. Rev. Lett. **81**, 4656 (1998).
[26] Y. Xia, Y. Ma, Y. Xing, Y. Mu, C. Tan, and L. Mei, Phys. Rev. B **61**, 11088 (2000).

[27] A. N. Kolmogorov and V. H. Crespi, Phys. Rev. Lett. **85**, 4727 (2000).
[28] Y. Ma, Y. Xia, M. Zhao, R. Wang, and L. Mei, Phys. Rev. B **63**, 115422 (2001).
[29] L. A. Girifalco and R. A. Lad, J. Chem. Phys. **25**, 693 (1956).
[30] L. Henrard, E. Hernández, P. Bernier, and A. Rubio, Phys. Rev. B **60**, R8521 (1999).
[31] M. Damnjanović, I. Milošević, T. Vuković, and R. Sredanović, Phys. Rev. B **60**, 2728 (1999).
[32] J. P. Lu, Phys. Rev. Lett. **79**, 1297 (1997).